

Uniaxial tensile test integrated design considering mould-fixture for UHPC

Xiaochen Zhang¹, Chao Shen², Xuesen Zhang³, Xiangguo Wu^{*4,5},
Qiu Faqiang⁶ and Josue G. Mitobaba¹

¹School of Civil Engineering, Harbin Institute of Technology, Harbin, 150090, China

²Shanghai Fengling Renewables Co., Ltd. Shanghai 200021, China

³CGN New Holdings Co., Ltd, Beijing 100070, China

⁴College of Civil Engineering, Fuzhou University, Fuzhou, 350108, China

⁵Key Lab of Structures Dynamic Behavior and Control of the Ministry of Education, Key Lab of Smart Prevention and Mitigation of Civil Engineering Disasters of the Ministry of the Industry and Information Technology, Harbin Institute of Technology, Harbin, 150090, China

⁶JianYan Test Group Co., Ltd, Xiamen 361004, China

(Received July 13, 2021, Revised December 24, 2021, Accepted January 4, 2022)

Abstract. Tensile property is one of the excellent properties of ultra-high performance concrete (UHPC), and uniaxial tensile test is an important and challenging mechanical performance test of UHPC. Traditional uniaxial tensile tests of concrete materials have inherent defects such as initial eccentricity, which often lead to cracks and failure in non-test zone, and affect the testing accuracy of tensile properties of materials. In this paper, an original integrated design scheme of mould and end fixture is proposed, which achieves seamless matching between the tension end of specimen and the test fixture, and minimizes the cumulative eccentricity caused by the difference in the matching between the tension end of specimen and the local stress concentration at the end. The stress analysis and optimization design are carried out by finite element method. The curve transition in the end of specimen is preferred compared to straight line transition. The rationality of the new integrated design is verified by uniaxial tensile test of strain hardening UHPC, in which the whole stress-strain curve was measured, including the elastic behavior before cracking, strain hardening behavior after cracking and strain softening behavior.

Keywords: finite element analysis; mould integration; uniaxial tension; ultra-high performance concrete; test fixture

1. Introduction

Ultra-high performance concrete (UHPC) is the latest generation of cement-based composites, which has excellent mechanical properties. Different to normal concrete, due to the bridging effect of fiber, UHPC shows strain hardening properties in tension. The test methods, loading devices and specimen types have an important influence in the test results. Compared to indirect tensile test, although the method of uniaxial tensile test can best reflect the real tensile properties

*Corresponding author, Professor, E-mail: wuxiangguo@hit.edu.cn

of concrete and geotechnical materials (Graybeal 2015), uniaxial tensile test is the most challenging test of concrete and geotechnical materials among all mechanical material property tests, especially for tensile strain hardening UHPC. This is because there are usually torque and eccentric moment (Haeri and Sarfarazi 2016) for the traditional dog bone shaped specimens (Felekoglu and Keskinates 2016) and specimens embedded steel bars (Zhou and Qiao 2018, 2019) in the uniaxial tensile test of concrete and geotechnical engineering. In recent years, the setting of ball hinge assembly (Min *et al.* 2016) and the design of double guide rail tensile device (Meng *et al.* 2017) were used to reduce the influence of eccentricity in tensile test. Two stress uniformity indexes were put forward by Yang (2017) to evaluate the quality of the specimen size. The effect of specimen shape on tensile properties of UHPC was studied by (USBR 4914 1992, Cunha *et al.* 2011, Denarié *et al.* 2003, Graybeal 2006, Jun and Mechtrherine 2010, Li 1998, 1996, Naaman and Homrich 1989, Roth *et al.* 2010, Sujivorakul 2002, Zhang *et al.* 2000). The right size of UHPC tensile specimen was proposed by (Hassan *et al.* 2012). A new method of gripping system (rotating or fixed boundary condition) for uniaxial tensile test of UHPC was revised by Park and Wille (Park *et al.* 2012, Wille *et al.* 2014), which can measure the whole stress-strain curves.

However, in the uniaxial tensile test, the difference between mould and fixture is inevitable, which becomes one of the influencing factors of cumulative eccentricity. There is an inherent initial gap between the fixture and the end of the specimen, which is easy to cause local stress concentration and the cracks often do not occur in the test zone. To solve this problem, integrated analysis and design of mould and fixture is studied in this paper. The end of mould is used as the one part of fixture, which realizes the seamless matching between the end of the specimen and the fixture. The methods were verified by test. The test results proved the feasibility and effectiveness of the integrated design of the multi-functional mould and fixture.

2. Test setup

2.1 Design thought

The uniaxial tensile test design of UHPC mainly includes the determination of specimen shape and size, and the design of fixture.

2.1.1 Specimen shape and size

The shape of uniaxial tensile specimens includes prismatic specimen, cylindrical specimen and dog bone specimen with and without notch. For prismatic specimen and cylindrical specimen, specimens are usually bonded to the fixture by adhesive. For prismatic specimens and cylindrical specimens without notch bonded to the fixture in the end (Cunha *et al.* 2011, Denarié *et al.* 2003, Haeri and Sarfarazi 2016, Komurlu *et al.* 2017), as shown in Fig. 1, it is more effective to measure the elastic behavior before cracking. However, considering the limited interfacial tensile strength between specimen and fixture, bond failure often occurs, which makes it difficult to measure the strain hardening behavior in tensile test (Denarié *et al.* 2003). The strain hardening properties can be obtained for prismatic specimens without notch when specimens are bonded to the fixture on the side, as shown in Fig. 2 (Roth *et al.* 2010, Zhang *et al.* 2000). However, the measurement length should be long enough to be away from the end restraint.

For notched specimens, local failure occurs due to stress concentration. This is different from the failure stress state of the specimen under uniaxial tension, and is not suitable for measuring the

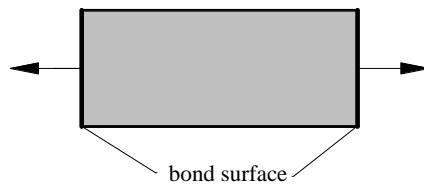


Fig. 1 End-glued unnotched specimen (Cunha *et al.* 2011, Denarié *et al.* 2003, Haeri and Sarfarazi 2016, Komurlu *et al.* 2017)

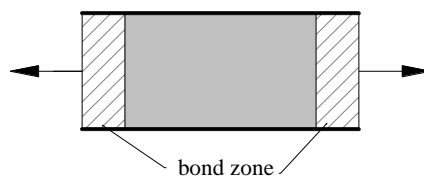
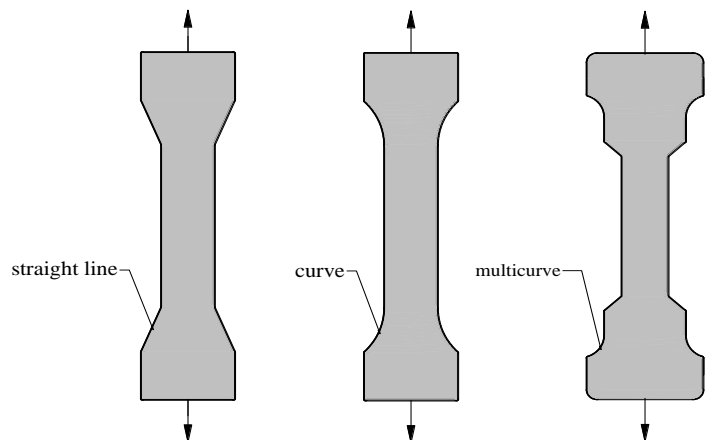


Fig. 2 Side-glued unnotched specimen (Denarié *et al.* 2003)



(a) Straight line type
(Cunha *et al.* 2011)

(b) Curve type
(Zhang *et al.* 2000)

(c) multicurve type
(Roth *et al.* 2010)

Fig. 3 Transition zone shape of dog bone specimen

elastic or strain hardening properties. In addition, if the notch height is not enough, it will not be conducive to the formation of multi crack failure.

Compared with cylinder specimen and prism specimen, the middle straight section of dog bone specimen can be designed with different length, which is convenient to observe multiple cracks and average crack spacing, and can measure the elastic, hardening and softening section of UHPC tensile properties. So, dog bone specimen is more suitable to be used for tensile test. According to the shape of the transition zone between the end and the middle straight line, the dog bone specimen can be divided into straight line type, curve type and multicurve type, as shown in Figs. 3(a)-3(c) respectively. In this paper, the straight-line dog bone specimen is used for the uniaxial tensile test.

When the size effect is not considered, the minimum dimension of UHPC specimen should be at least twice of the maximum fiber length to ensure the random distribution of fibers (Hassan *et al.* 2012).

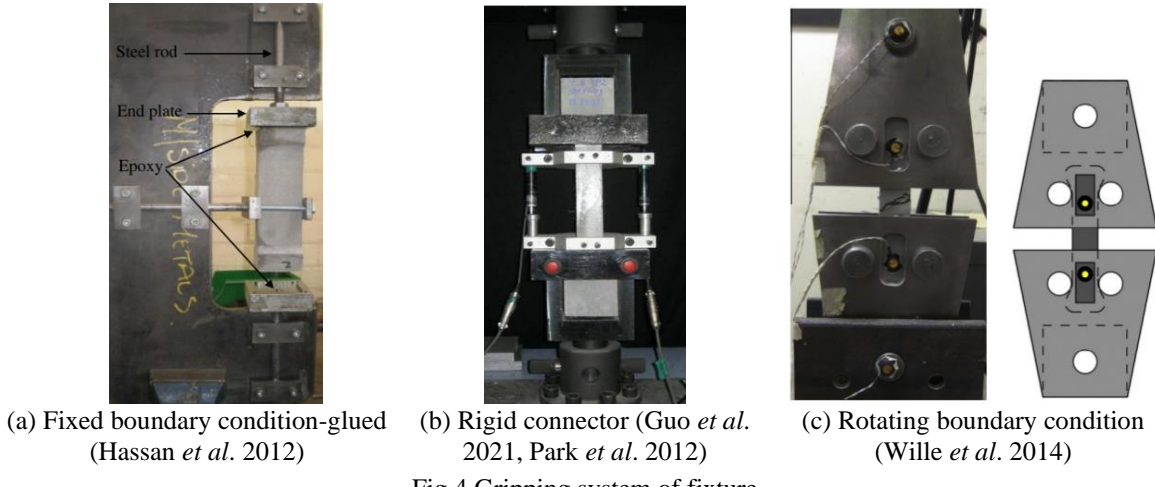


Fig.4 Gripping system of fixture

2.1.2 Gripping system of fixture

According to the boundary condition between fixture and the testing machine, the gripping system of fixture can be divided into rotating and fixed boundary condition. The specimen is usually glued to the steel plate (Hassan *et al.* 2012) (see Fig. 4(a)) to achieve the fixed boundary condition. Besides, a rigid connector is added to connect with the experimental machine (Guo *et al.* 2021, Park *et al.* 2012), as shown in Fig. 4(b) to achieve the fixed boundary condition. The rotating boundary condition is achieved by hinge restraint, shown in Fig. 4(c). For the fixed boundary condition, the initial eccentricity and additional bending moment are often caused by the fabrication error of the specimens. For the rotating boundary condition, the contact area between the specimen and the fixture is small, which causes the stress concentration at the end of specimen.

In this paper, the dog bone shaped specimen is chosen as the specimen of the uniaxial tensile test. The middle straight zone is long enough to ensure the formation of multiple cracks, The end is amplification to reduce the stress. Through the integrated design of mould and fixture, the seamless matching between the specimens and the fixture is realized. The rotating boundary condition was chosen in this paper.

2.2 Composition of mould and fixture

The multi-functional integrated mould and fixture are shown in Fig. 5(a). The mould and fixture are shown in Figs. 5(b) and 5(c), respectively. The part "1" in the figure is the bottom plate of the mould, which should have a big enough rigidity to ensure that the bottom surface of the specimen is flat, part "2" is the side plate of the mould, which should also have a big enough rigidity, part "3" is the end of the mould, which can also be used as the fixture in the tensile test, and its strength and rigidity should meet the requirements of deformation and strength for the tensile test. Part "4" is the pull rod to connect the experimental fixture with the experimental machine, which should be selected according to experimental machine, part "5" is the connecting plate, which is used to connect the pull rod and the experimental fixture. The parts "6" and "7" are pin bolts to be used for the rotating boundary condition. The part "9" is bolt to fix the bottom plate

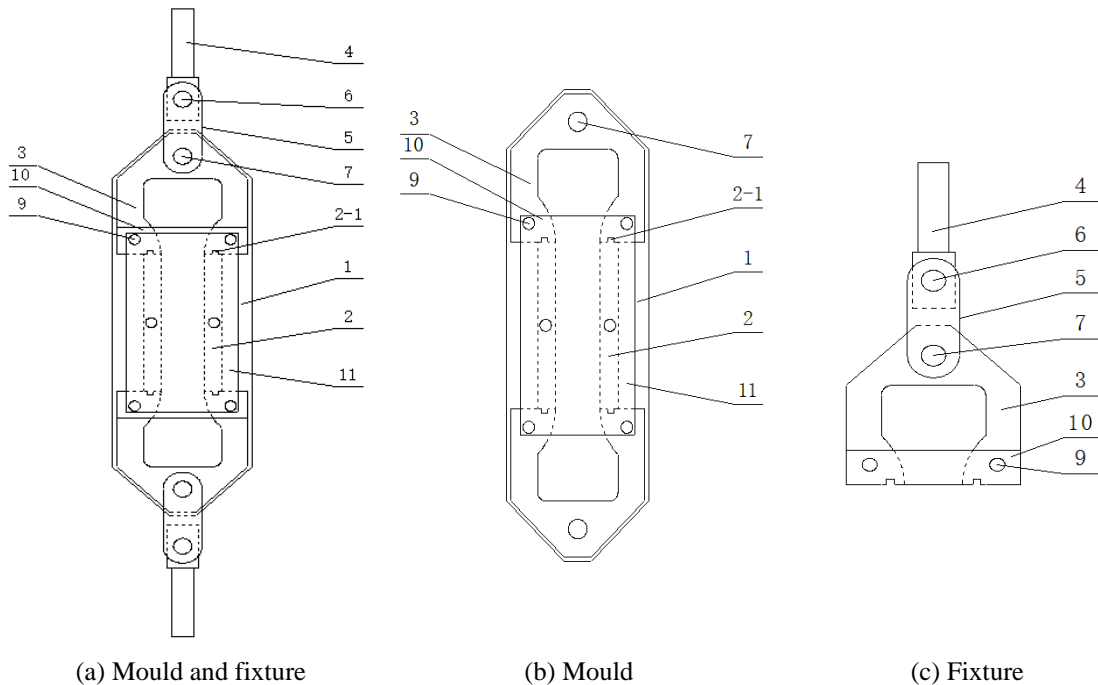


Fig. 5 Multi-functional uniaxial test setup

and side plate of mould, The part “10” is a transverse steel plate, which is mainly to prevent the transverse deformation caused by insufficient strength and stiffness of fixture. Therefore, the transverse steel plate is used as a transverse constraint to ensure the “perfect” matching between fixture and specimen surface. The part “11” is a thin plate as a top surface of mould, avoiding the influence of eccentricity caused by the roughness of the upper surface. In addition, several additional gaskets, named component “8”, should be added to ensure the connecting plates “5” are parallel to the surface of the test specimen.

2.3 Connection

In order to ensure the relative position of the side plate and the end of the specimen mould are horizontally concentric, a shear key is set, as shown in “2-1” (Fig. 5(b)). For the bolts used to connect the bottom plate and the side plate, the bolt’s holes should be small, and the bolts should be half button bolts, that is, only half of the bolts have screws, and the rest of the sections are smooth screws. The gasket size of part “8” should be reasonably selected to ensure that the bottom and top surface of specimens are parallel to the plane of connecting plate “5”. It is suggested to add a positioning device on the bottom plate, such as positioning pin key, to fix the side plate.

2.4 Force analysis of test fixture

The fixture is the most complex part for the multi-functional mould and fixture in the tensile test. The stress distribution of fixture under tension is analyzed by the finite element method (FEM). Then, the fixture is optimized according to the FEM result.

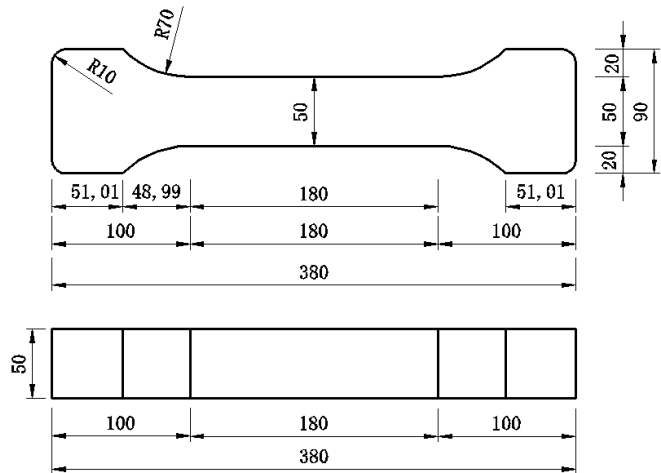


Fig. 6 specimen sizes



Fig. 7 UHPC and molds

3. Modeling analysis

Usual steel fiber (the size with length of 13 mm and the diameter of 0.2 mm) for UHPC was used in this paper. The size of specimen selected in this paper is shown in Fig. 6 according to the suggestion of USBR 4914 (1992). The cross-section size of the middle straight section of the dog bone shaped specimen is 50 mm × 50 mm and 180 mm in length, which can make sure the fiber is free distribution in the three-dimension, and the length can meet the condition of multiple cracks.

3.1 Parameters analysis

In order to reasonably select the transition zone between the middle straight-line zone and the end amplification zone, firstly, the single curve radius R of 70 mm and the straight-line transition were compared. Then, it is also necessary to investigate the extrusion restraint effect between the fixture and the specimen. To improve the efficiency of the analysis, in the finite element modeling analysis, one end of the specimen is tied with fixture to analyze the effect of single curve transition form, and the other end is free without fixture to investigate the effect of fixture on the specimen.

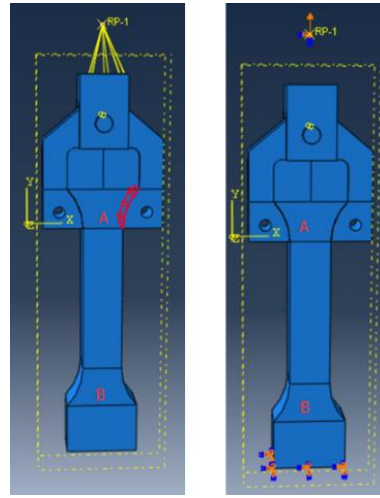


Fig. 8 Constraints and loading methods

3.2 Process

3.2.1 Material

Steel is selected as elastic material, and the yield strength of steel is 355MPa. UHPC is elastic-plastic material, and the tensile strength of UHPC assumes 20MPa, which is big enough to make sure the fixture is not destroyed in real tensile test.

3.2.2 Modeling of UHPC and steel fixture

Solid element C3D8R is used for fixture and UHPC material. The UHPC and fixture with single curve transition are shown in Fig. 7. The end A of the specimen is connected with the fixture. And the boundary condition at the end B of the specimen is fixed to the ground.

3.2.3 Interface contact and constraints

The interface contact between the end A of the specimen and the fixture is constrained by surface friction and the friction coefficient is 0.4. The boundary condition of the end B of the specimen is fixed to the ground (Fig. 8).

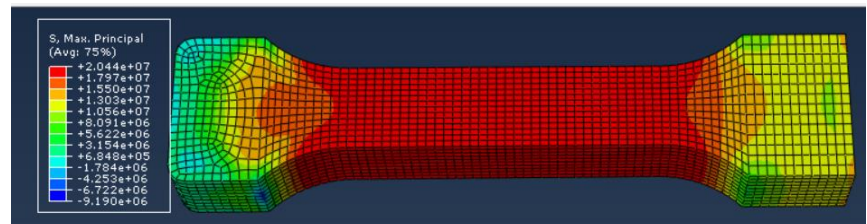
3.2.4 Loading

The vertical displacement load with constant speed of displacement is applied at RP-1 point. When the maximum principal stress of the element in the middle straight-line zone reaches the tensile strength, the test is broken off.

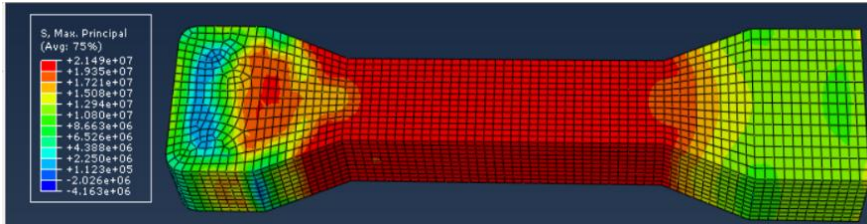
4. Results

4.1 Maximum principal stress

Due to the contact between the curve transition of the specimen and the fixture, the end A of the UHPC specimen is in biaxial stress state without considering the friction between the interfaces.



(a) Curve transition



(b) Straight line transition

Fig. 9 Maximum principal stress

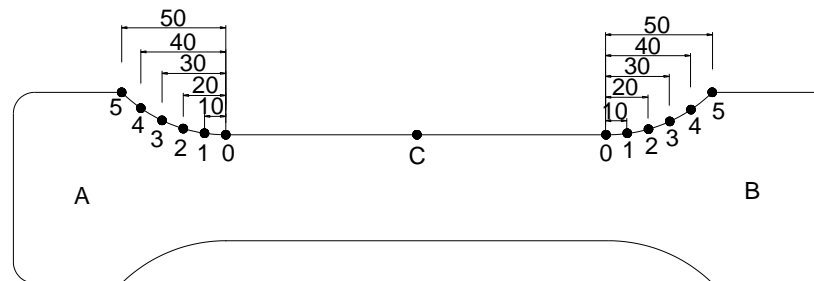
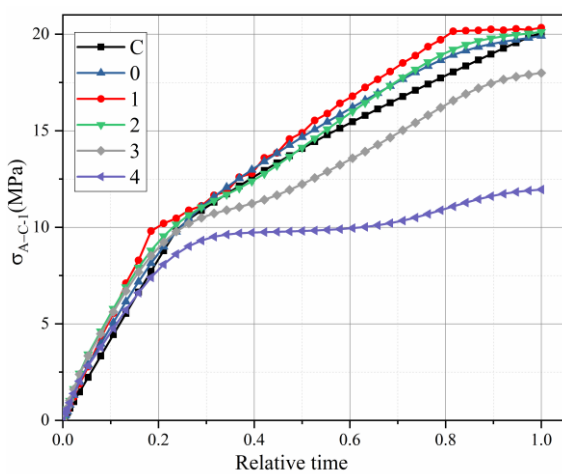
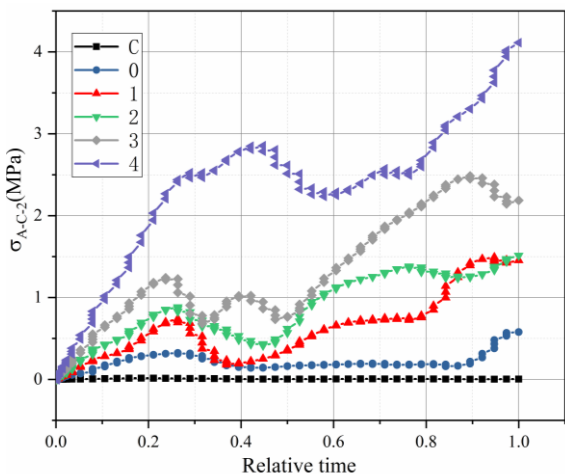


Fig. 10 Definition of points



(a) Maximum principal tensile stress



(b) The middle principal tensile stress

Fig. 11 the principal stress of end A with curve

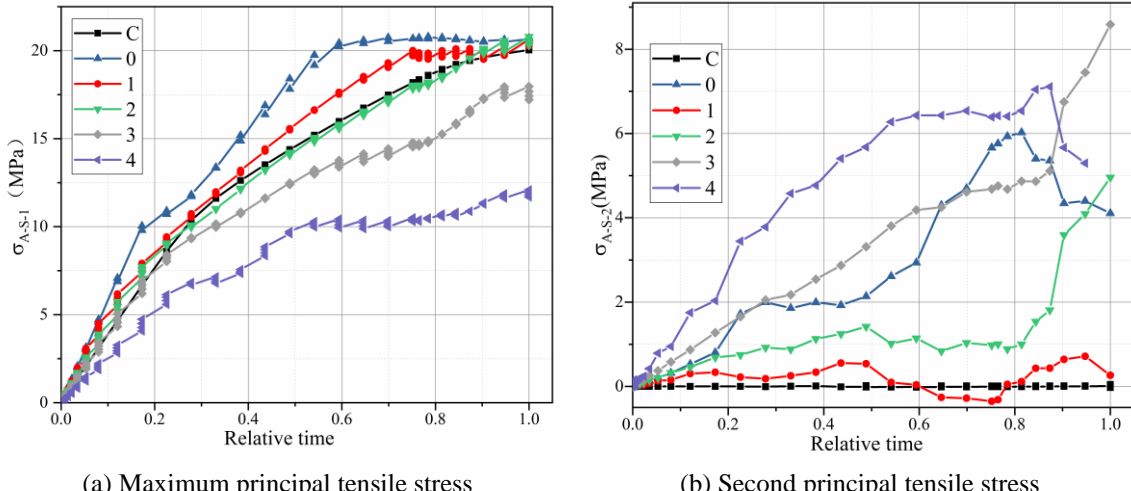


Fig. 12 the principal stress of end A with straight line

The stress state of specimens when the middle straight line reaches the set ultimate tensile strength, is shown in Fig. 9.

4.2 The effect of curve transition on the principal stress

As shown in Fig. 10, the meaning of each point in the curve transition zone of the specimen indicates the distance from the intersection of the curve and the middle straight-line zone.

As shown in Figs. 11 and 12, when the transition zone at the end A is a straight line (S) or curve (C), except for point “5” (where the cross-sectional area is larger than other points and the maximum principal stress is negative, i.e., in the compression state), the transition zone at end A of the specimen is biaxial tensile. Therefore, according to the fact that the biaxial tensile strength of concrete under biaxial tension is equal to the uniaxial tensile strength, only the maximum principal tensile stress needs to be compared.

According to the analysis results, when the transition zone is a straight line (S), there is stress concentration, and at the points “A-0” and “A-1”, the stress of the straight line transition is greater than that of the curve transition, that is, the curve transition is preferred the straight line transition. However, even if the curve transition is chosen, it can't guarantee that the maximum principal stress of each point in the transition zone is much greater than that in the middle straight section because the cross section just increased a little. And there is still the possibility of failure outside the test zone.

4.3 Effect of fixture on the maximum principal stress

For the end B without fixture, the specimen is in unidirectional tensional state, so only the maximum principal stress of each point needs to be compared. As shown in Figs. 13 and 14, the maximum principal stress at each point increases with the loading.

When the maximum principal stress at the middle straight zone reaches the tensile strength, the maximum principal stresses at the other points are shown in Table 1. The results show that the

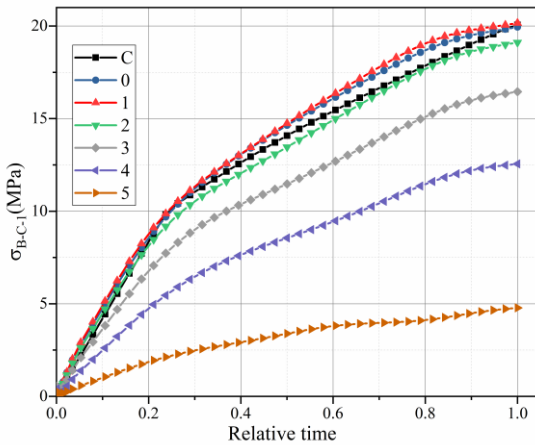


Fig. 13 The max. principal stress of end B with curve

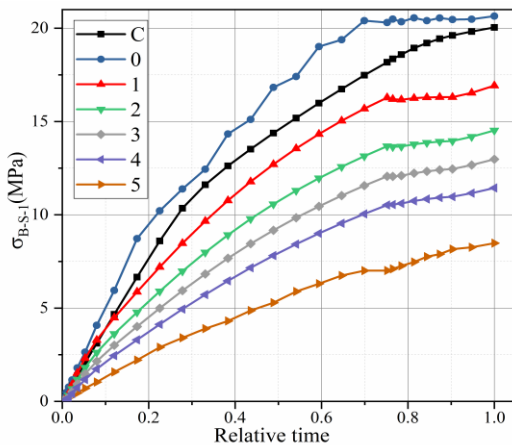


Fig. 14 The max. principal stress of end B with straight line

fixture has a certain influence on the maximum principal stress of the specimen, and the greater the distance from the middle straight line, the greater the influence. Therefore, considering the convenience of the experimental operation and the reasonable stress distribution of the specimen, it is suggested to adopt the fixture with curve transition.

5. Application to verify

5.1 Preparation of integrated mould and fixture

The size of the test specimen is shown in Fig. 15. The thickness of the specimen is 50 mm. The wire cutting method is used for operating steel fixture. To ensure that the end part of mould and the middle side strip can be installed precisely, it is suggested that the convex key of the side strip should be smaller than the design size, and the end groove should be larger. In order to ensure that

Table 1 The max. principal stress

Position	Middle straight zone	A-C-0	A-C-1	A-C-2	A-C-3	A-C-4	A-C-5
The max. principal stress (MPa)	20	20.2	20.28	20.25	19.78	15.49	-4.83
Position	Middle straight zone	A-S-0	A-S-1	A-S-2	A-S-3	A-S-4	A-S-5
The max. principal stress (MPa)	20	20.68	20.55	19.76	14.51	10.72	-2.38
Position	Middle straight zone	B-C-0	B-C-1	B-C-2	B-C-3	B-C-4	B-C-5
The max. principal stress (MPa)	20	20.19	20.18	19.27	16.53	12.37	5.52
Position	Middle straight zone	B-S-0	B-S-1	B-S-2	B-S-3	B-S-4	B-S-5
The max. principal stress (MPa)	20	20.61	17.64	14.93	13.38	11.87	8.44

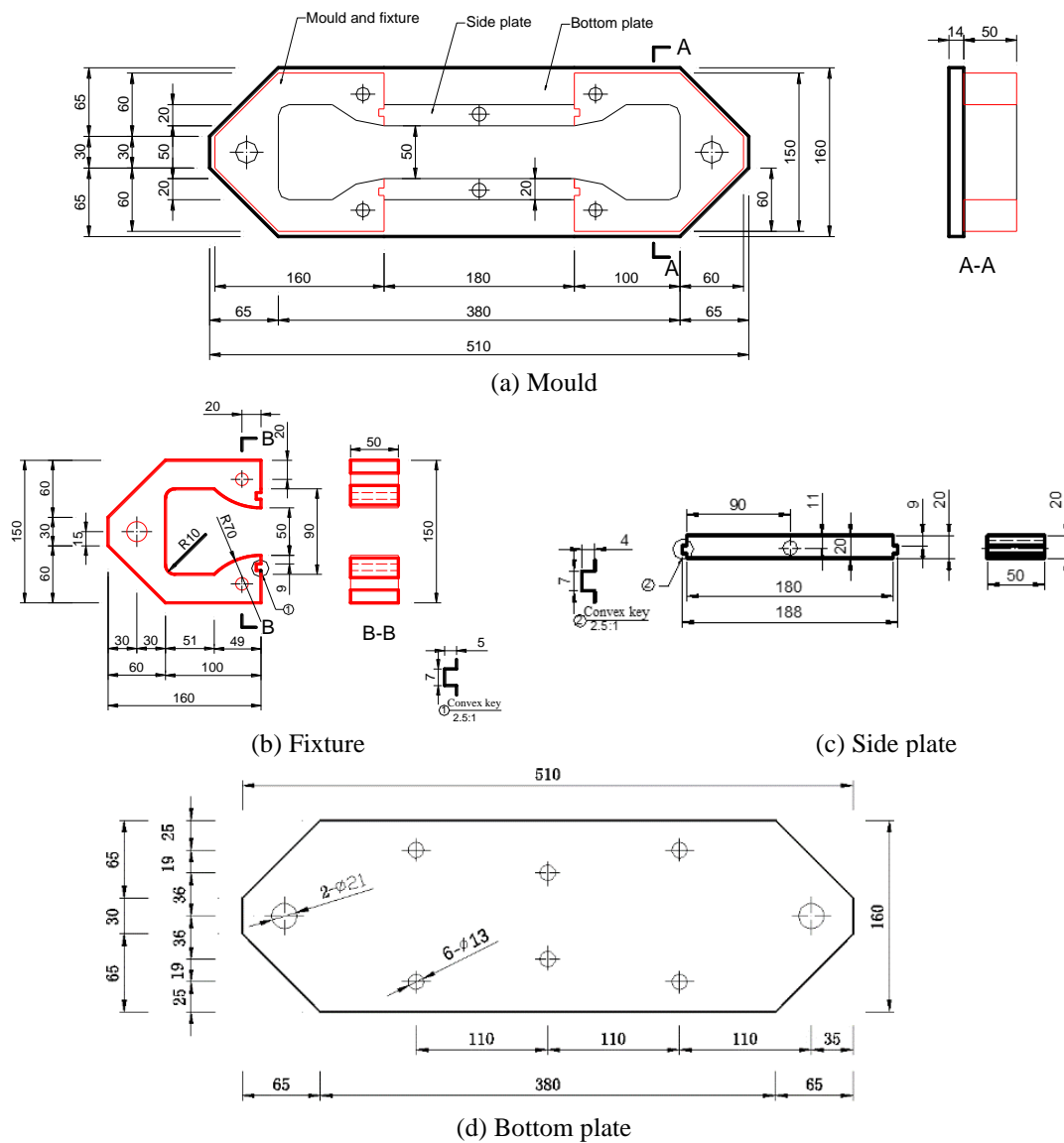


Fig. 15 Sizes of multi-functional uniaxial tests setup



Fig. 16 Test setup and steel constraint

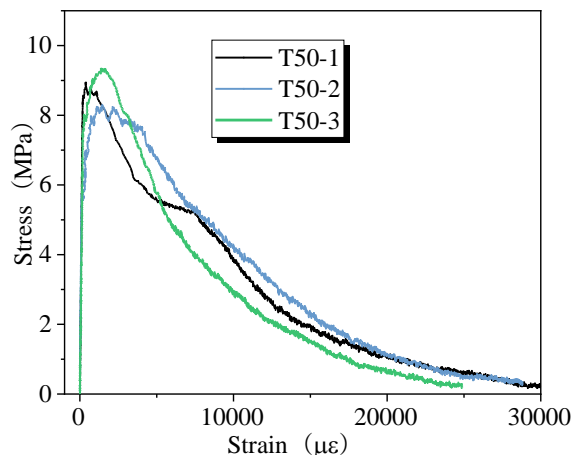


Fig. 17 Tensile test result

the specimen made of the mold can meet the design requirements, the locating pin key should be added in the local area, for example, the locating key should be set at the two ends of mould. The dimensions of each part of the mould are shown in Fig. 15.

5.2 Confirmatory test

A reasonable connection device to connect the experimental machine and the fixture should be selected to make sure that the fixture can rotate before tensile test. For example, the experimental machine can be connected with the fixture through a pin bolt, as shown in Fig. 16. And a connecting device is composed by two steel plates and two pin bolts, which is simple and convenient to assemble.

The principal tensile crack of UHPC is in the middle measuring zone, as shown in Fig. 16. The

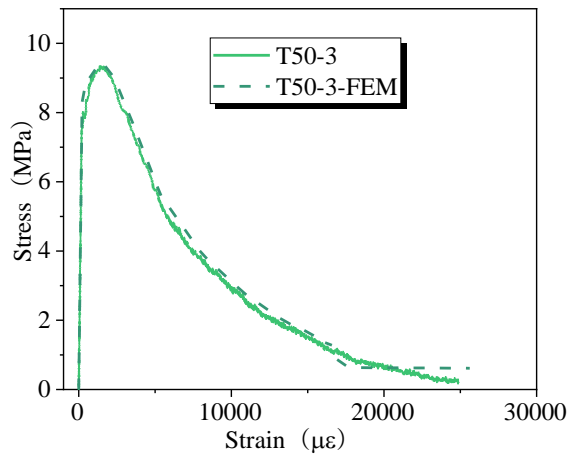


Fig.18 Results of test and FEM

test results are shown in Fig. 17. The whole stress-strain curve was measured, including the elastic behavior before cracking, strain hardening behavior after cracking and strain softening behavior, which confirms that the integrated mould and fixture are effective for tensile test of UHPC. Furthermore, the stress-strain curve of specimen T50-3 was simulated by FEM to compare with the test result, as shown in Fig. 18. which indicates that the result of FEM agrees well with the test result.

6. Conclusions

In this paper, an integrated scheme of mould and fixture for tensile test is proposed. Finite element analysis, processing application, and feasibility verification of the scheme are carried out. The main finding can be recapitulated as follow:

- The finite element analysis shows that when the transition zone is a straight line, there is stress concentration, and the stress of the straight line transition is greater than that of curve transition. It is suggested that the curve transition mode should be preferred.
- The fixture has a certain influence on the maximum principal stress of the specimen, and the greater the distance from the middle straight line zone, the greater the influence. Considering the convenience of operation and the rationality of stress, it is suggested to adopt single curve transition.
- The integrated mould and fixture for tensile test, can achieve the function of automatic centering and rotation in the experiment, which ensures that the measuring area of the specimen is in the single axis tension state, and the experimental installation is convenient.

Acknowledgement

This work was supported by the National Natural Science Foundation of China (grant number 52178195), and the Xiamen Construction Science and Technology plan project (XJK2020-1-9).

References

- Cunha, V.M., Barros, J.A. and Sena-Cruz, J.M. (2011), “An integrated approach for modelling the tensile behaviour of steel fibre reinforced self-compacting concrete”, *Cement Concr. Res.*, **41**(1), 64-76. <https://doi.org/10.1016/j.cemconres.2010.09.007>.
- Denarié, E., Habel, K. and Brühwiler, E. (2003), “Structural Behaviour of Hybrid Elements with Advanced Cementitious Materials (HPFRCC)”, *Proceedings of the 4th International workshop on high performance fiber reinforced cement composites, HPRFCC-4*, Ann Arbor, Michigan, U.S.A., June.
- Felekoglu, B. and Keskinates, M. (2003), “Multiple cracking analysis of HTPP-ECC by digital image correlation method”, *Comput. Concr.*, **17**(6), 831-848. <https://doi.org/10.12989/cac.2016.17.6.831>.
- Graybeal, B.A. (2006), “Material property characterization of ultra-high performance concrete”, Research Report No. FHWA-HRT-06-103, Federal Highway Administration, Office of Infrastructure Research and Development, U.S.A.
- Graybeal, B.A. (2015), “Tensile mechanical response of ultra-high-performance concrete”, *Adv. Civil Eng. Mater.*, **4**(2), 62-74. <https://doi.org/10.12989/anr.2018.6.3.279>.
- Guo, M, Gao, R. (2021), “Experimental comparability between steam and normal curing methods on tensile behavior of RPC”, *Adv. Concr. Constr.*, **11**(4), 347-356. <https://doi.org/10.12989/acc.2021.11.4.347>.
- Haeri, H. and Sarfarazi, V. (2016), “Numerical simulation of tensile failure of concrete using particle flow code (PFC)”, *Comput. Concr.*, **18**(1), 39-51. <https://doi.org/10.12989/cac.2016.18.1.039>.
- Hassan, A.M.T., Jones, S.W. and Mahmud, G.H. (2012), “Experimental test methods to determine the uniaxial tensile and compressive behaviour of ultra high performance fibre reinforced concrete (UHPFRC)”, *Constr. Build. Mater.*, **37**(12), 874-882. <https://doi.org/10.1016/j.conbuildmat.2012.04.030>.
- Jun, P. and Mechtcherine, V. (2010), “Behaviour of strain-hardening cement-based composites (SHCC) under monotonic and cyclic tensile loading: part 1—experimental investigations”, *Cement Concr. Compos.* **32**(10), 801-809. <https://doi.org/10.1016/j.cemconcomp.2010.07.019>.
- Komurlu, E., Kesimal, A. and Demir, A.D. (2017), “Dog bone shaped specimen testing method to evaluate tensile strength of rock materials”, *Geomech. Eng.*, **12**(6), 883-898. <https://doi.org/10.12989/gae.2017.12.6.883>.
- Li, V.C. (1998), “Engineered cementitious composites (ECC)-tailored composites through micromechanical modeling”, Research Report No. MI 48109-2125, Advanced Civil Engineering Materials Research Laboratory, Department of Civil and Environmental Engineering, University of Michigan, Ann Arbor, U.S.A.
- Li, V.C., Wu, H.C., Maalej, M., Mishra, D.K. and Hashida, T. (1996), “Tensile behavior of cement-based composites with random discontinuous steel fibers”, *J. Am. Ceram. Soc.*, **79**(1), 74-78. <https://doi.org/10.1111/j.1151-2916.1996.tb07882.x>.
- Meng, C., Shang-yu, H. and Bao-ning, H. (2017), “Development and application of a new geotechnical device for direct tension test”, *Rock Soil Mech.*, **38**(6), 1832-1840.
- Min, C., Yuchen, S. and Qiao Z. (2016), “An investigation on intrinsic stress-strain relationship of concrete subjected to static and dynamic uniaxial tension”, *Mater. Rev.*, **30**(8), 118-121.
- Naaman, A.E. and Homrich, J.R. (1989), “Tensile stress-strain properties of SIFCON”, *Mater. J.*, **86**(3), 244-251.
- Park, S.H., Kim, D.J., Ryu, G.S. and Koh, K.T. (2012), “Tensile behavior of ultra high performance hybrid fiber reinforced concrete”, *Cement Concr. Compos.*, **34**(2), 172-184. <https://doi.org/10.1016/j.cemconcomp.2011.09.009>.
- Roth, M.J., Eamon, C.D., Slawson, T.R., Tonyan, T.D. and Dubey, A. (2010), “Ultra-high-strength, glass fiber-reinforced concrete: Mechanical behavior and numerical modeling”, *ACI Mater. J.*, **107**(2), 185-194.
- Sujivvorakul, C. (2002), “Development of high performance fiber-reinforced cement composites using twisted polygonal steel fibers”. Ph.D., Dissertation, University of Michigan. Ann, Arbor, U.S.A.
- USBR 4914. (1992), “Procedure for direct tensile strength, static modulus of elasticity, and poisson’s ratio of

- cylindrical concrete specimens in tension”, Bureau of United States Department of InteriorReclamation.
- Wille, K., El-Tawil, S. and Naaman, A.E. (2014), “Properties of strain hardening ultra high performance fiber reinforced concrete (UHP-FRC) under direct tensile loading”, *Cement Concr. Compos.*, **48**(2), 53-66. <https://doi.org/10.1016/j.cemconcomp.2013.12.015>.
- Yang, J., Chen, B.C. and Shen, X.J. (2018), “The optimized design of dog-bones for tensile test of ultra-high performance concrete”, *Eng. Mech.*, **35**(10), 37-46.
- Zhang, J., Stang, H. and Li, V.C. (2000), “Experimental study on crack bridging in FRC under uniaxial fatigue tension”, *J. Mater. Civil Eng.*, **12**(1), 66-73.
- Zhou, Z. and Qiao, P. (2018), “Direct tension test for characterization of tensile behavior of ultra-high performance concrete”, *J. Test. Evaluat.*, **48**(4), 2730-2749. <https://doi.org/10.1520/JTE20170644>
- Zhou, Z. and Qiao, P. (2019), “Tensile behavior of ultra-high performance concrete: Analytical model and experimental validation”, *Constr. Build. Mater.*, **201**, 842-851. <https://doi.org/10.1016/j.conbuildmat.2018.12.137>.

TK